A concept for accurate edge-coupled multi-fiber photonic interconnects

A concept for accurate edge-coupled multi-fiber photonic interconnects

M. H. M. van Gastel, P. C. J. N. Rosielle, and M. Steinbuch, *Fellow*, *IEEE*

***Abstract*—The alignment and fixation of multiple single-mode optical fibers to photonic integrated circuits is currently a challenging, expensive and time-consuming task. In this paper, we present a concept for a sub-micrometer accurate multi-fiber array where fibers are actively aligned with respect to each other and fixated to a flat carrier using UV-curable adhesive. Adhesives are prone to shrinkage which can disturb the fiber alignment. As a result, especially the fixation process forms the bottleneck in reaching the required alignment and not the alignment process itself. Simulations are performed to investigate the sensitivity of process variables on the adhesive bond geometry which is important for the shrinkage amplitude. Furthermore an experimental setup has been designed and fabricated to measure the shrinkage induced fiber displacement for three selected types of adhesives. The results show a controllable adhesive shrinkage where fibers can be aligned with a position reproducibility of ± 40 nm which is more than sufficient for the most critical fiber alignment applications. With this concept an important step can be made in enabling sub-micrometer accurate photonic interconnects in a cost effective way which is suitable for automated production.**

***Index Terms*—Optical fiber array, fiber-optic alignment, packaging, UV-curing adhesives.**

I. Introduction

Assembly and packaging is becoming an increasingly important issue for photonic integrated circuits (PICs). For single-mode edge-coupled optical chips especially the fiber alignment and fixation has been a bottleneck in terms of product performance, cost and production volume. Planar waveguide devices with small mode field diameters (MFD) require a lateral alignment accuracy in the order 0.1 μm to achieve an acceptable insertion loss [1]. The assembly and packing is the most expensive phase in the manufacturing process, estimated at $>$50% of the overall cost of any fiber-optic device.

Passive alignment methods, based on mechanical alignment features, such as placing fibers in etched V-grooves [2], are often preferred due to their intrinsic simplicity. However, due to geometrical fiber tolerances, especially the core-cladding eccentricity, the required alignment accuracy cannot be met using these methods. As a result, active alignment methods, based on the feedback of an optical signal, are often employed. By measuring the transmitted optical power while moving the fiber using a high precision actuator, the required alignment accuracy can be met. The current applied techniques are however time-consuming, expensive, not easily automated and often not applicable for multi-fiber interconnect due to a large footprint [3], [4]. In this paper an alignment and assembly approach is proposed which addresses these issues. For this concept first an array is manufactured where individual fibers are actively aligned with respect to each other and fixated using an UV-curable adhesive with a resulting < 0.1 μm accurate mutual alignment of the fiber cores. Subsequently, this array can be aligned and fixated to the optical chip. In this paper we focus on the assembly of the fiber array.

We start by introducing the proposed optical fiber array concept and by discussing its properties and advantages over the current solutions. The adhesive fixation of the fibers is the most critical component of the proposed concept regarding the alignment accuracy since adhesives are prone to curing shrinkage, which results in fiber displacements after alignment. In Section III the adhesive fiber fixation will be investigated in more detail. Simulations are performed to investigate the sensitivity of the bond geometry for varying adhesive volumes and fiber-substrate distances and the corresponding meaning concerning shrinkage shifts will be discussed. To investigate the positional stability of the adhesive bond, an experimental setup is designed and built which will be discussed in detail. Using this setup the fiber displacements during the curing process for three types of adhesives for varying process parameters are measured. In addition the speed of the fixation process and stability of the bond is investigated experimentally. Finally, the results of these experiments are discussed and the feasibility of the proposed array concept is shown.

II. Proposed optical fiber array concept

The main challenge to obtain a low loss coupling in PICs is to overcome the accuracy bottleneck due to the core eccentricity of the individual fibers. In the proposed concept the alignment is separated into two steps. First a fiber array is assembled with a mutual lateral alignment accuracy of < 0.1 μm between the fiber cores. Later on this fiber array is assembled in one step to the PIC. With this decoupled approach we eliminate the risk of discarding an entire chip when a fiber alignment has failed. Additionally, this allows for dedicated assembly equipment, resulting in a faster and more economical production.

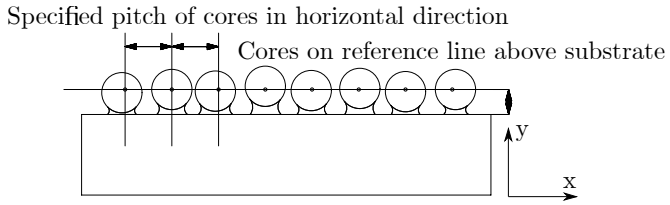

Fig. 1: The proposed concept of the optical fiber array.

Fig. 1 visualises the proposed fiber array concept. The array consists of multiple single-mode fibers which are fixated to a

flat Quartz carrier substrate using UV-curable adhesive. Each fiber is individually actively aligned with respect to the already fixated fibers using a high-precision manipulator before curing. The adhesive layers are used to overcome differences in core-cladding eccentricities. During the alignment process the cores of the fibers are positioned with no variation in vertical direction on a horizontal line above the substrate and with a predefined pitch in horizontal direction. By using an adhesive as fixation method, the achievable distance between the fibers can be kept to a minimum since the adhesive only needs to be present at a small portion of the fiber diameter. The fiber pitch is only limited by the outer diameter of the fiber and on the tolerances of the fiber core position. Since fiber core-eccentricities are small, typical ± 1 μm, the adhesive layer thickness can be kept small such that the vertical shrinkage can be minimized. Moreover, a smaller adhesive thickness is preferred due to an increased bond stiffness and a decreased sensitivity for thermal expansions. The usage of a simple flat carrier without the need for any electrical connections or mechanical adjustments results in a cost effective solution where the number and pitch of the fibers can be easily varied for specific chip designs. In addition, multiple types of fibers, such as Polarization-maintaining and lensed fibers can be combined onto one carrier. Both loose fibers and fiber ribbons can be used as input in the proposed concept without fundamental limitations. Due to the relatively small footprint of this array in comparison with other methods, it can be integrated more easily into a package. Fused Quartz is selected as material of the carrier substrate since it has the same coefficient of thermal expansion (CTE) as the Fused Silica of the optical fibers, $0.55 \cdot 10^{-6}$ K^{-1}. This results in minimal thermal stresses and introduced coupling losses when the temperature changes. The Fused Quartz light transmission range of 310-2000 nm allows for UV-curing from below the substrate. By curing from beneath the substrate, a homogeneous illuminated bond is obtained which prevents fiber tilts due to uneven curing over the length of the bond profile. UV-curing adhesives are preferred over thermal-curing adhesive to obtain fast processing speeds and less thermal disturbance during the alignment and fixation process. To create optical interconnects at the other side of the array, the opposite fiber ends should be attached to, for example, a connector. Since the alignment tolerances are usually more relaxed for this side of the fibers due to a larger MFD, passive alignment methods or standard connectors could be used prior or after the assembly of the proposed array. We aim to obtain a lateral alignment accuracy of < 0.1 μm for an acceptable insertion loss. The bottleneck in achieving this accuracy in present solutions is especially the fixation process and not the active alignment process itself [5], [6]. Adhesives are prone to shrinkage during or after the curing process, which causes misalignment after the final bonding step. The amplitude of this shrinkage should either be 1) small enough to obtain the desired alignment accuracy, or 2) the adhesive shrinkage should be repeatable such that an offset can be applied before the curing process. To investigate this in more detail simulations and experiments are performed. Simulations are performed on the bond geometry for different fiber-substrate distances and adhesive volumes.

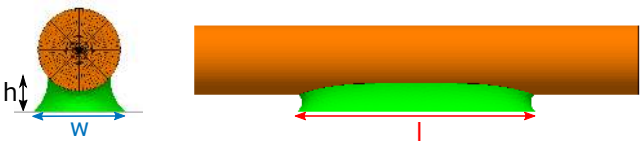

Fig. 2: Front- and sideview of the evolved Surface-Evolver model.

These simulations are important to study the effect of process variables on the variability of the adhesive bond and consequently the shrinkage behaviour. Existing multi-fiber V-groove arrays have the advantage of an entirely passive alignment in a quick batch process. The array concept proposed in this work relies on active alignment. The main advantage of this concept over the existing passive solutions is the ability to compensate for production tolerances of both the fibers and the substrate. Simultaneously, the proposed concept is flexible in the number and pitch of fibers. Due to these tolerances, passively aligned V-groove arrays are limited to a typical ± 1.0 μm mutual fiber alignment, which results in undesirable coupling losses for interconnects to small MFD devices such as InP PIC.

III. Adhesive joint geometry

The magnitude and direction of the shrinkage of the adhesive is determined by two factors: 1) the chemical properties of the adhesive, and 2) the adhesive bond geometry. Furthermore the bond strength and thermal expansion are also dependent on this geometry. The wetting of the adhesive droplet between the fiber and substrate is not bounded by mechanical features such as with V-groove arrays, but is solely determined by surface tension and hydrostatic pressure. The software package Surface Evolver [7] is used to simulate the geometry to investigate the sensitivity of the bond for a varying fiber-substrate distance and adhesive volume. Surface Evolver evolves the surface to its minimum-energy shape. In Fig. 2 the model is visualised. The material properties and parameters of a typical selected UV-adhesive (contact angles: $\theta_{fib/subs-adh} = 40°$, surface tension: $\gamma = 0.037$ N/m) are used for the simulations. More details on the selected adhesives can be found in Sec. IV-C. The initial horizontal droplet position with respect to the fiber is varied in the simulations to not only account for exact axis-symmetric droplet dispensing.

A. Simulation results

The minimum surface energy is reached for a bond geometry which shows a vertical symmetry with respect to the fiber as shown in Fig. 2. No or negligibly small disturbance is therefore expected for the fiber alignment in horizontal direction during a homogeneous cure. The variation of the initial horizontal droplet position shows no effect on the bond geometry and is therefore not further discussed. The bond geometry shows furthermore a large aspect ratio between the width and length of the droplet. In Fig. 3 the results are visualised for the bond geometry, i.e. height, width (left figure) and length (right), as function of adhesive volume for a fixed fiber-substrate distance of z=3 μm. For increasing adhesive volumes the geometry shows an increasing trend in

all direction where in particular the droplet will spread in its length direction (Fig. 3, right). The slope of the curves in Fig. 3 gradually levels off for larger volumes which corresponds to the cylindrical shape of the fiber. Since the amplitude of the vertical shrinkage is directly dependent on the adhesive thickness, the results indicate that for larger volumes (V$>$ 800 pL) the sensitivity for variation in dispensed adhesive volume decreases. In Fig. 4 the simulation results are visualized for the bond geometry as function of the fiber-substrate distance (z in Fig. 2) for a fixed droplet volume of V=1000 pl. The results show that for decreasing fiber-substrate distances the droplet will spread in the length direction where the droplets width and height decreases. The curve of the droplets length shows a rapidly increasing slope for smaller fiber-substrate distances. The curves of the droplets width and height both show a more linear trend as function of the distance. The slope of these both curves decreases for smaller fiber-substrate distances. Since the amplitude of the vertical shrinkage is directly dependent on the adhesive thickness, an almost linear trend for the shrinkage amplitude is expected as function of the fiber-substrate distance. The decreasing slope of the droplet height as function of the fiber-substrate distance indicate the preference for smaller fiber-substrate distances. A variation in fiber-substrate distance will than likely less affect the amplitude of the vertical shrinkage. Next to simulations, experiments are performed to investigate the fiber drift due to adhesive shrinkage as function of the fiber-substrate distance. An experimental setup is therefore designed and built.

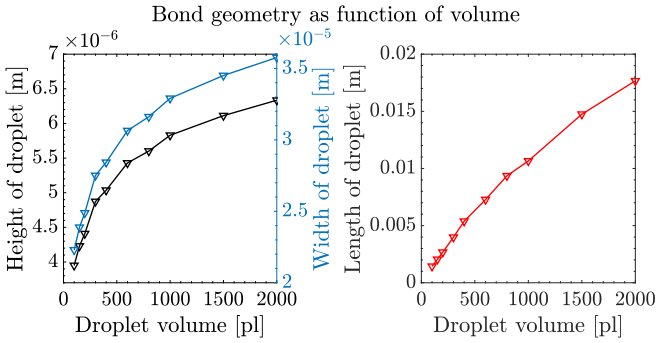

Fig. 3: Surface-Evolver simulation of the bond geometry as function of volume for a fixed fiber-substrate heigth z=3 μm.

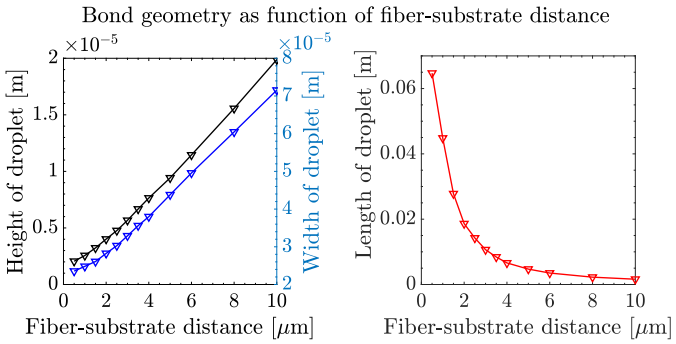

Fig. 4: Surface-Evolver simulation of the bond geometry as function of the fiber-substrate distance for a fixed droplet volume of V=1000 pL.

IV. Experimental setup

An experimental setup is designed to investigate the feasibility of the proposed fiber array concept regarding the position stability and repeatability of the curing process for different types of adhesives and process parameters.

In Fig. 5 the experimental setup is visualized. The setup is able to accurately measure the shrinkage during the curing process for an adjustable fiber-substrate distance. To vary the fiber-substrate distance, a flexural mechanism is designed which can translate over a stroke of $\pm$185 μm in vertical direction. A single-mode fiber ($\varnothing$125 μm) is held in this mechanism using an integrated vacuum V-groove gripper. The geometry of the V-groove passively aligns the fiber with respect to the other components of the setup. The flexural mechanism consists of a parallelogram structure which is actuated using a differential micrometer with a 1:6 lever. This results in backlash-free motion with a resolution of $u \approx$ 0.12 μm, which is sufficient to set a repeatable fiber-substrate distance. To measure the displacement, an inductive probe (Mahr Millimar 1301) is integrated on top of the mechanism. A CCD camera (Basler acA640-90um) is placed in front of this flexural mechanism to capture the curing process. A translation stage is used to focus the camera with respect to the front surface of the fiber. Underneath the flexural mechanism a substrate holder is present where the substrate is supported on two outer edges. The substrate holder is placed onto two translation stages to align the droplet with the fiber in horizontal direction and to place the fiber and droplet in the same focus field of the camera. A rectangular cutout is present in the holder to enable UV-curing from underneath the substrate. For the UV-curing a 365 nm LED Spot Curing System (Omnicure LX500) is used to minimize thermal input during the measurements. The different components are fixated to a stiff frame with a calculated lowest eigenfrequency of 1200 Hz to maintain the mutual position. To reduce the influence of external disturbances, the whole setup is placed onto a vibration isolated table.

A. Fiber position measurement

To measure the position of the fiber core during the curing process, a measurement is performed relative to two already fixated reference fibers. A low power laser source (2.5 mW, 635 nm) is used to launch light into the single-mode fibers. The beams emitted from the fiber and references are focused onto the CCD camera using a microscope lens and aspheric lens. The image is subsequently processed in Matlab. The emitted laser beams approximately have a Gaussian intensity distribution and therefore a Gaussian least-squares-fit is used to extract the pixel-positions of the fibers. To relate the pixel-position to displacements, a calibration step is performed. In this calibration the fiber-end is displaced using the flexure mechanism over a range of $\pm$185 μm in 20 steps. A linear calibration is obtained using a least-square-estimate between the pixel position and real-life displacement of the fiber using the inductive probe with a 3σ repeatability smaller than 0.1 μm. This calibration process is repeated for each measurement. Measurements are performed relative to two reference fibers

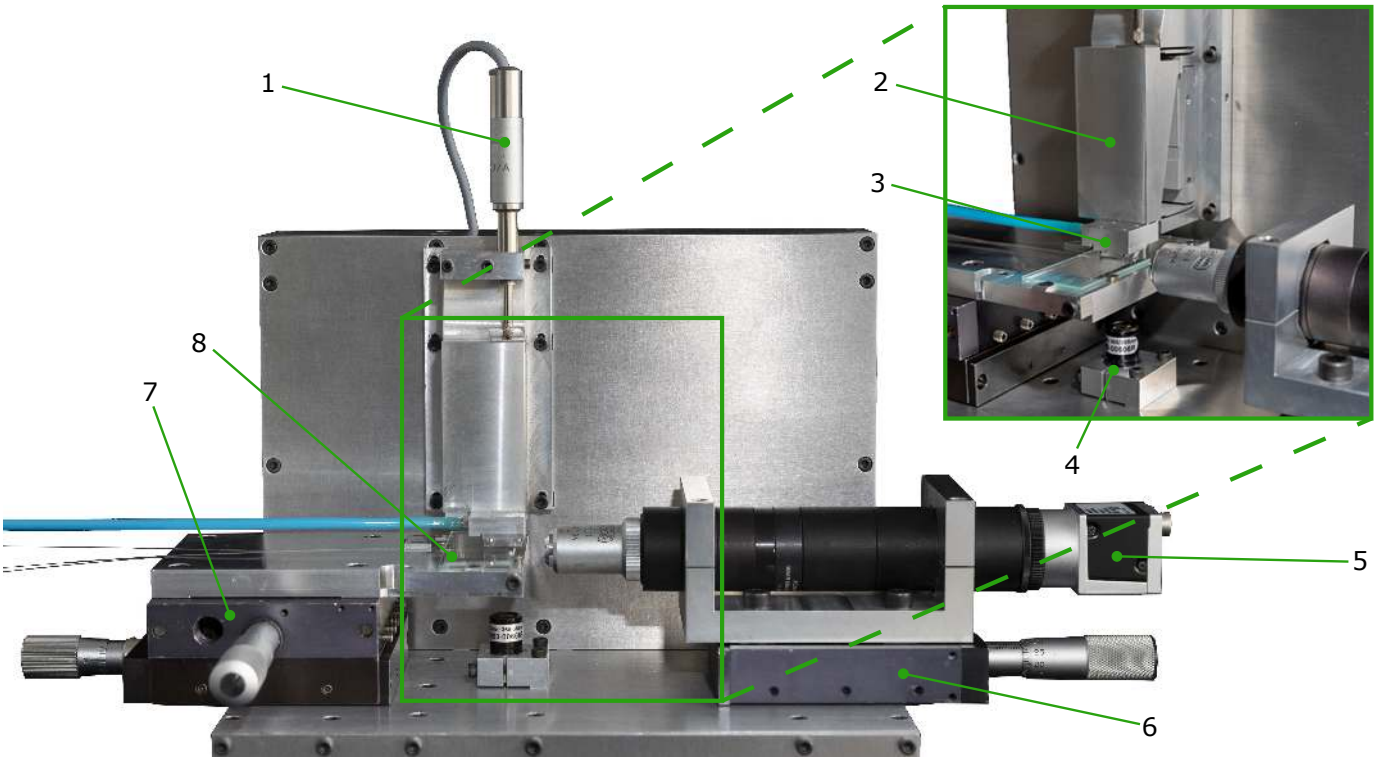

Fig. 5: Overview of the experimental setup.

1) Inductive displacement probe
2) Flexural fiber manipulator
3) Vacuum fiber gripper
4) LED UV-curing head
5) Microscope camera
6) Translation stage for camera focusing
7) Positioning stages for substrate
8) Substrate with fixated reference fibers

which are fixated to the substrate. This results in a short measurement loop which eliminates sources of errors such as movements of the substrate or flexure mechanism, e.g. due to thermal expansion. In Fig. 6 the front surface of three fixated fibers and the corresponding emitted laser spots are visualised. Using camera feedback for alignment, the position to obtain optimal alignment is instantly known and therefore the process time can be significantly reduced compared to other active alignment procedures which are based on optical power measurements. In the latter case, first the emitted light has to be localized and subsequently a complex alignment process has to be started since the movement direction of the fiber to obtain the optimal alignment is unknown. When directly coupling individual fibers to waveguides on the PIC, an absolute alignment is required which does not allow the use of a camera. However, as the fibers of the array have to be mutually aligned a camera can be used, which significantly reduces the most time-consuming part of the alignment process. Hereby, only for the final alignment of the entire array to the PIC, an optical power measurement has to be used.

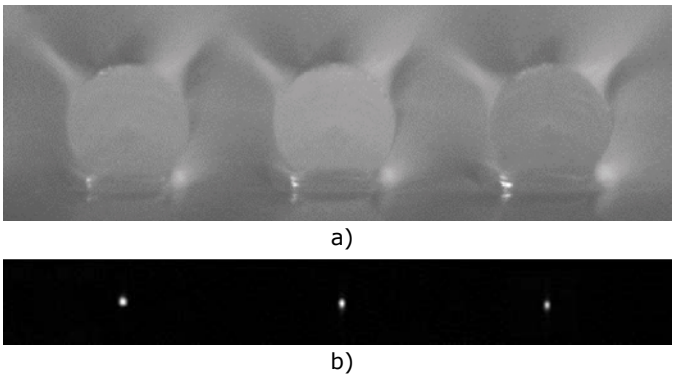

Fig. 6: Typical end face images of fixated fibers, a) when laser is turned off, b) when laser is turned on.

B. Procedure

In Fig. 7 a block diagram of the measurement procedure is visualised. Before each measurement batch, the Quartz substrate is rinsed and cleaned from contaminations using Isopropanol (IPA) in an ultrasonic cleaner. Single-mode fibers with a diameter of 125 μm are used for the experiments. For each measurement, the fiber-end is stripped from the plastic covering, cleaned using IPA and cleaved before placement in the vacuum gripper. A pin transfer process is used to dispense adhesive droplets of $V \approx 1000$ pl on the substrate. After the adhesive dispensing, the substrate is loaded into the substrate holder. The fiber is subsequently placed into

the droplet and the fiber-substrate distance is set using the flexural mechanism. Hereafter the adhesive is cured and the displacement is measured. Before each measurement batch, two fibers are fixated to the substrate as reference.

C. Adhesive selection

Three types of adhesives are selected for the experiments: Summer Lens Bond SK9, Nordland Optics 61 and 81. In Table I an overview of the key adhesive properties, as specified by the manufacturers, is visualised. All selected adhesives have a low shrinkage upon cure which is necessary to provide a long term dimensional stability and to minimize curing stress. Furthermore adhesive are selected which have a relatively high modulus of elasticity to provide a stiff connection with the substrate, yet being compliant enough to accommodate stresses due to differential expansion. The Telcordia GR-1209-CORE standard for passive optical components requires a temperature range between $-40°C$ and $85°C$. Therefore adhesives are selected with a small CTE, to minimize the difference with the silica/quartz of the fiber and substrate, and a high glass transition temperature. Other considered adhesive properties are the viscosity and surface tension for dispensing and wetting, strength/adhesion to glass, curing times and water absorption, which should be minimal for dimensional stability.

V. Experimental results and Discussion

The experimental results of the three selected adhesives are discussed in this section.

A. Typical time-response

An example of the measured fiber displacements during the curing process is visualised in Fig. 8. In this figure the displacements of the fiber to be cured is visualised relative to the two already fixated reference fibers. When the UV head

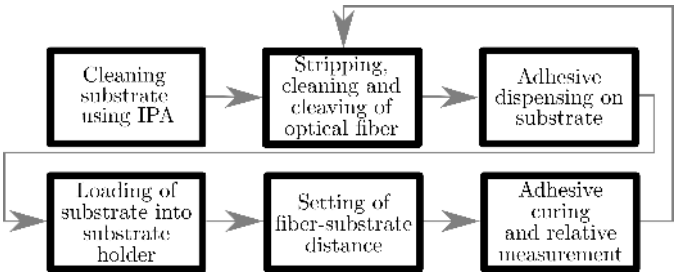

Fig. 7: Block diagram of the measurement procedure.

TABLE I: Key material properties of the selected adhesives.

	NOA 81	NOA 61	SK9
E-modulus [GPa]	1.4	1.1	2.8
Linear shrinkage	N/A	1.5%	0.25%
CTE [$°C^{-1}$]	N/A	$25{\cdot}10^{-5}$	$7{\cdot}10^{-5}$
Tg [°C]	125	125	100
Water absorption	N/A	0.16%	0.8%

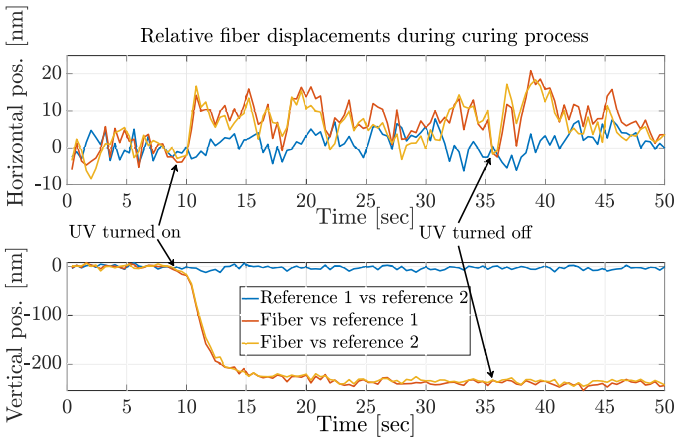

Fig. 8: Measured fiber displacements during the adhesive curing process.

is turned on a vertical displacement (Fig. 8, lower plot) is observed for the fiber to be cured as a result of the adhesive shrinkage. The velocity of this displacement increases to a constant when the light is turned on and then decreases again to zero when the adhesive is cured. As expected with a vertical symmetrical bond profile, no significant (< 10 nm) horizontal displacement (top plot) is observed during the curing process. The reference fibers show a negligible (< 10 nm) mutual displacement during the curing process.

B. Shrinkage measurement results

To measure the shrinkage of the selected adhesives, the fiber to substrate distance is varied between 1 to 3 μm in discrete steps of 1 μm using the flexure mechanism. This selected range is sufficient to overcome the most typical core-eccentricity amplitudes. Larger adhesive layers are unfavorable due to a lower bond stiffness and an increased sensitivity for temperature induced displacements. For each combination of adhesive and fiber to substrate distance, the experiment is repeated 10 times to identify the sensitivity and repeatability of the process. Figure 9 shows the results of the adhesive shrinkage experiments. In this figure the solid blue lines represent the linear least-squares fit through the black measurement points. The dashed blue lines represent the 3σ-prediction bounds of this fit. The horizontal displacement upon curing is not shown since all results show no significant fiber displacement in this direction (< 10 nm) as also observed in the time-response of Fig. 8.

A negative linear trend can be observed for the shrinkage as function of the fiber-substrate distance for all considered adhesives. The amplitude of the vertical fiber displacement upon curing has a value between 100-220 nm which is in general too large to achieve the required alignment accuracy. However since the repeatability of the process is high with 3σ-prediction bounds in the range of $\pm$35-40 nm, an offset to the position of the fiber can be applied before curing to reach the desired alignment. The slope of the linear least-squares fit through the measurements points is relatively gentle: $\approx$ 30-40 nm vertical shrinkage per μm fiber-substrate distance. This gentle slope of the shrinkage curve results in a, favorable,

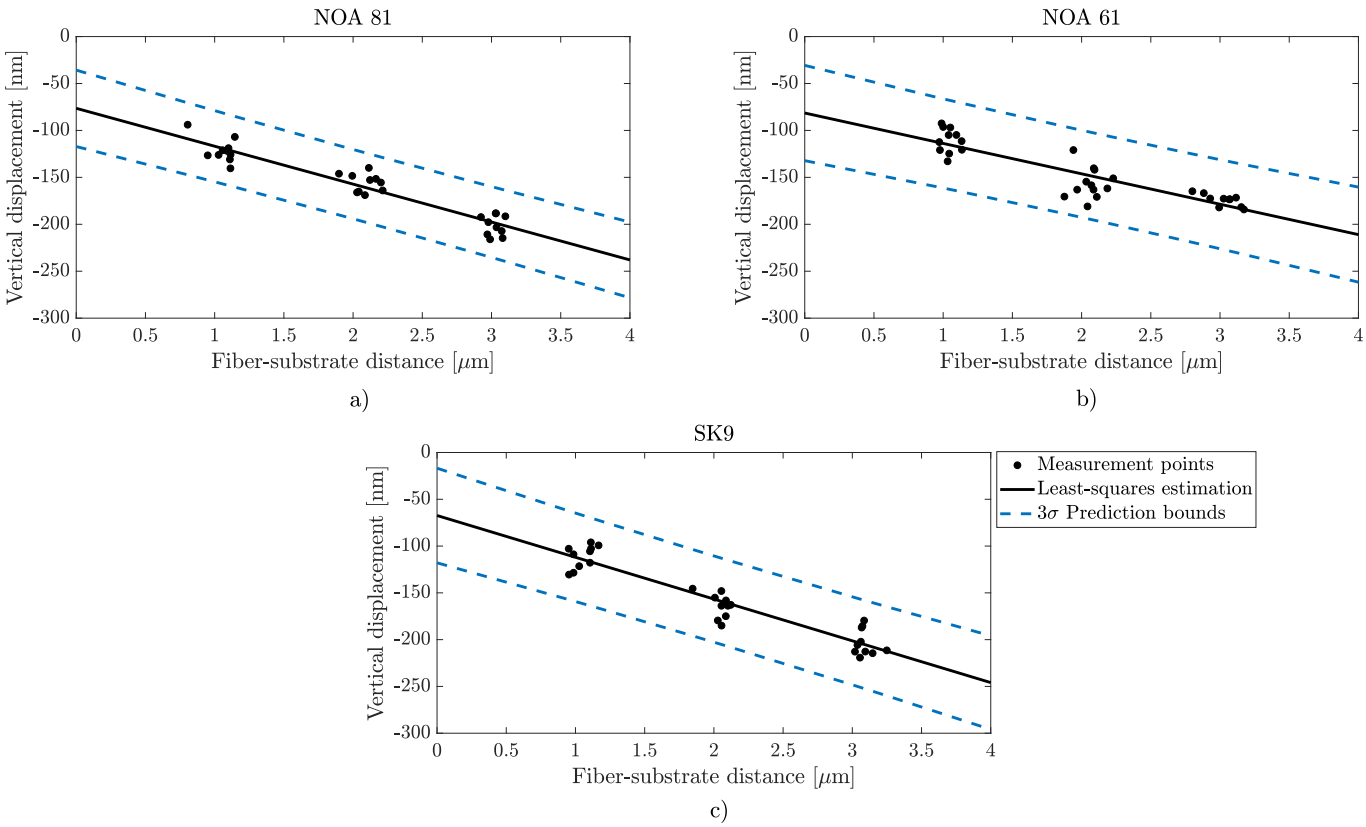

Fig. 9: The vertical fiber displacement due to adhesive shrinkage as function of the fiber-substrate distance for three adhesives. a) NOA 81. b) NOA 61. C) SK9.

small sensitivity of the process for a varying fiber core-eccentricity. The observed linear trend corresponds well with the simulation results of Fig. 4 where also a near linear trend of the adhesive height/shrinkage was predicted. The predicted decreasing slope of the shrinkage as function of the fiber-substrate distance is however not visible. This is probably caused by a too small decrease in slope with respect to the measurement uncertainty. The fit of the experimental results shows a negative displacement for a zero fiber-substrate distance. In reality this will not be true since the fiber is unable to descent through the top surface of the substrate. This is likely caused by the geometry of the adhesive bond around the fiber. The adhesive is situated higher on the circumference of the fiber than the minimum fiber-substrate distance as shown in the simulation results in Fig. 4. This results in a higher shrinkage than predicted based on the minimum fiber-substrate distance until the fiber beds down on the substrate. Experiments performed with near zero, decreasing, fiber-substrate distances confirm this hypothesis with decreasing fiber displacements until the fiber beds down on the substrate and no fiber displacement is measured.

C. Curing times

A fast processing speed is desired for an automated volume-production of fiber arrays. Therefore the curing times of the adhesives considered is investigated experimentally as function of the UV-intensity. The curing time is defined as the time after no movement is detected of the fiber during curing. For optimal bond strength a post-cure could be necessary to obtain full cross-linking of the polymer chains. The results in Fig. 10 show an exponential decreasing curing time as function of an increasing light intensity for all adhesives considered. This indicates that a certain activation energy is required to start the reaction and that after a certain intensity, the maximum chemical reaction speed is reached [8]. After a threshold, higher UV-intensities will therefore not result in a significant decrease in curing time. For low UV-intensities the SK9 adhesive cures significantly faster than the two other considered adhesives. For higher intensities the differences in curing speed between the adhesives diminishes to a small value. The amplitude of the adhesive shrinkage shows no influence on the UV-intensity which permits high UV-intensities for a faster curing time. A cure in less than 5 seconds is possible for a UV-intensity of 2 W/cm^2. This is a relative short fixation time when compared to other fixation/alignment methods typically used in active alignment procedures such as laser forming and welding, which can take up to 25 seconds [9].

D. Discussion

In Table II an overview of the measurement results is visualised. No significant differences in the measurement results are observed between the adhesives considered. The aimed lateral alignment accuracy of < 0.1 μm can be met with all adhesives considered. All adhesives show an adequate bond strength to overcome the basic forces acting on the fibers. This bond strength is however insufficient to meet the

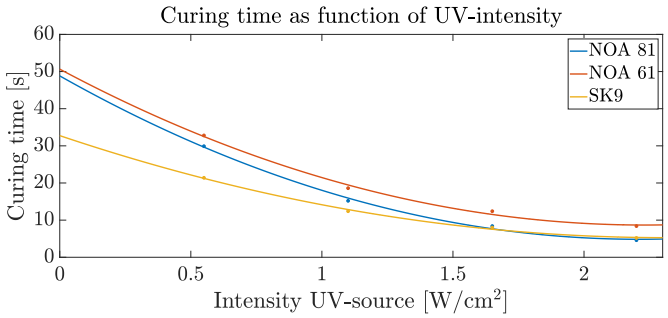

Fig. 10: Curing time as function of UV-intensity.

TABLE II: Overview of the measurement results.

Adhesive type	**Adhesive shrinkage** [nm/μm]	3σ **Prediction bound** [nm]	**Curing time at** 2 W/m^2 [s]
NOA 81	40.4	$\pm$35.6	5.2
NOA 61	32.4	$\pm$42.9	8.4
SK9	44.6	$\pm$45.2	4.3

Telcordia 1209 standard. A secondary, larger, adhesive droplet is therefore applied at approx. 5 mm axial distance from the primary fixations without disturbing the fibers' position. Using this strain relief the fiber itself will fail before the adhesive fixation both in a straight pull and side pull fiber test. When the shrinkage measurement results are compared to the manufacture supplied specifications of Table I, a discrepancy is observed: 4.5% vs. 0.25% for SK9, and 4.3% vs. 1.5% for NOA61, respectively. The most likely explanation for this discrepancy is the specific bond geometry in the experiments in comparison with the standard samples employed by the manufactures. As shown in Fig. 4, the adhesive spreading results in a thin bond with a large ratio of both width and length to height. In the work of Lewoczko-Adamczyk *et al.* [10], it is reported that for this type of bond geometry, all of the volumetric shrinkage occurs in the height/vertical direction of the bond. As a result, a larger percentage shrinkage is observed for samples with a smaller gap. In addition, since no standard sample and measurement technique for shrinkage is used, the specified values between manufacturers can also have a different meaning.

VI. Conclusion

In this paper a new concept for a sub-micrometer accurate edge-coupled fiber array has been proposed. The proposed concept results in a cost effective, flexible solution where pitch, number and type of fiber can be varied without changing the manufacturing process. Contrary to traditional passive fiber arrays, the use of adhesive layers compensates for differences in core cladding eccentricities between the fibers. The stability and shrinkage upon cure of this adhesive fixation is the most critical and uncertain aspect of the concept and therefore investigated using simulations and experiments. Simulations of the geometry of the bond show that for larger adhesive volumes the sensitivity for variation in dispensed adhesive volume decreases indicating the preference for larger adhesive volumes. Furthermore a near linear shrinkage was predicted as function of the fiber-substrate distance. An experimental setup is designed and built to measure the position stability and repeatability of the curing process for three types of adhesives. The experimental results for layer thicknesses of 1-3 μm, show vertical fiber displacements in the range of 100-220 nm and no horizontal fiber displacements due to presumably the symmetrical bond geometry. A 3σ-prediction bound of $\pm$35-40 nm is reported for the reproducibility of the process showing the feasibility of sub-micrometer accurate mutual fiber alignment. Due to this high reproducibility an offset to the position of the fiber can be applied before curing to reach the desired alignment. No significant differences are observed in the measurement results between the adhesives considered. Curing times of less than 5 seconds are measured and combined with camera-based active alignment this shows advantages over traditional active alignment methods regarding process time. This concept shows its promise by making sub-micrometer accurate photonic interconnects available in a cost effective way. To make this concept applicable in real world the next step is to automate the manufacturing process.

References

[1] G. Böttger, H. Schröder, and R. Jordan, "Active or passive fiber-chip-alignment: Approaches to efficient solutions," in *Optoelectronic Interconnects XIII*, vol. 8630. International Society for Optics and Photonics, 2013, p. 863006.

[2] R. Hauffe, U. Siebel, K. Petermann, R. Moosburger, J.-R. Kropp, and F. Arndt, "Methods for passive fiber chip coupling of integrated optical devices," in *Electronic Components & Technology Conference, 2000. 2000 Proceedings. 50th*. IEEE, 2000, pp. 238–243.

[3] V. A. Henneken, W. P. Sassen, W. van der Vlist, W. H. Wien, M. Tichem, and P. M. Sarro, "Two-dimensional fiber positioning and clamping device for product-internal microassembly," *Journal of Microelectromechanical systems*, vol. 17, no. 3, pp. 724–734, 2008.

[4] J. H. van Zantvoort, S. G. Plukker, P. I. Kuindersma, K. A. Mekonnen, and H. de Waardt, "Mechanical devices for aligning optical fibers using elastic metal deformation techniques," *IEEE Transactions on Components, Packaging and Manufacturing Technology*, vol. 6, no. 11, pp. 1687–1695, 2016.

[5] S. Wang, H. Chan, C. Wang, C. Wang, J. Liaw, M. Sheen, J. Kuang, C. Chien, G. Wang, and W. Cheng, "Post-weld-shift in semiconductor laser packaging," in *Electronic Components and Technology Conference, 1999. 1999 Proceedings. 49th*. IEEE, 1999, pp. 1159–1163.

[6] U. H. Fischer-Hirchert, *Photonic Packaging Sourcebook: Fiber-Chip Coupling for Optical Components, Basic Calculations, Modules*. Springer, 2015.

[7] K. A. Brakke, "The surface evolver," *Experimental mathematics*, vol. 1, no. 2, pp. 141–165, 1992.

[8] C. Decker, F. Masson, and R. Schwalm, "How to speed up the uv curing of water-based acrylic coatings," *JCT research*, vol. 1, no. 2, pp. 127–136, 2004.

[9] G. Folkersma, "Laser forming for sub-micron adjustment: with application to optical fiber assembly," 2015.

[10] W. Lewoczko-Adamczyk, S. Marx, and H. Schröder, "Shrinkage measurements of uv-curable adhesives: An elegant method based on a laser distance sensor for in-situ measurements of the polymerization shrinkage," *Optik & Photonik*, vol. 12, no. 4, pp. 41–43, 2017.